

Partial Discharge Characteristics in Composite Insulation Systems with PPLP for HTS Cable

Y Kikuchi¹, K Yamashita¹, A Kumada¹, K Hidaka¹, K Tatamidani² and T Masuda²

¹ Department of Electrical Engineering and Information Systems, The University of Tokyo, Japan

² Sumitomo Electric Industries, Ltd. Osaka Japan

Email:kikuchi@hvg.t.u-tokyo.ac.jp

Abstract. The electrical insulation system of high-temperature superconducting (HTS) cable consists of liquid nitrogen ($N_2(l)$) and polypropylene laminated paper (PPLP). Partial discharge (PD) may occur in butt gaps of the insulation layers and its characteristics imply the insulation performance of HTS cables. $N_2(l)$ cooling system is installed in the power system and $N_2(l)$ will flow through the cables during the system operation. Filling the HTS cable with $N_2(l)$ in order to perform pre-shipment inspection is time-consuming and costly for cable manufacturers. Therefore, they are trying to find a cost effective method for pre-shipment inspections. One alternative is to use high pressure gaseous nitrogen ($N_2(g)$) instead of $N_2(l)$. This article investigates PD characteristics such as PD inception electric field (PDIE) and PD extinction electric field (PDEE) in butt gaps of HTS cables in 0.1 to 0.3 MPa $N_2(l)$ and 0.1 MPa to 1.0 MPa $N_2(g)$ environments. For assessing the surface/volume effects, PD characteristics are measured with changing the size of butt gaps. It turns out that PDIE and PDEE in $N_2(g)$ are linearly correlated with those in $N_2(l)$ at any gas pressure in our testing, and PDIE in 1.0 MPa $N_2(g)$ is almost 30% of that in 0.2 MPa $N_2(l)$. It suggests that PD characteristics in $N_2(l)$ can be extrapolated from those in $N_2(g)$.

1. Introduction

In order to cope with the power demand in urban areas, high temperature superconducting (HTS) cable has attractive performance. In Japanese urban areas the electricity demand is high, therefore HTS cable is an outstanding way to increase the transmission capacity of the electricity, as well as providing a substantial reduction in transmission losses, resulting in a lower CO_2 emission. Moreover the reactance of HTS cable is smaller due to its outer HTS conductor for magnetic shield. This small reactance contributes to the improvement of voltage and synchronous stability of power system [1].

In insulation design of HTS cable, it is inevitable to insert small gaps which are called butt gaps through PPLP® layer. If these gaps had not been inserted properly through PPLP®, the cable insulation layer would have torn by bending the cable. Butt gap should be considered as the weakest points in electrical insulation because PD may be generated in butt gap and it leads to degradation of electrical insulation performance. $N_2(l)$ /PPLP® composite insulation is adopted to the HTS cable because of their high dielectric strength and low dielectric loss. $N_2(l)$ coolant will be circulated in the cable after it is installed in power system. A pre-shipment insulation test is usually performed in the manufacturer before the shipment of cables. The pre-shipment inspection of HTS cable with whole



length cooled in $N_2(l)$ is not economically efficient and it would be preferable to find a more cost effective method for the pre-shipment inspection.

From the above background, the authors have been investigating the PD characteristics of $N_2(l)$ /PPLP® composite insulation system for HTS cable under ac-voltage application [2]. The authors have focused on the alternative inspection method conducted in $N_2(g)$ at room temperature instead of in $N_2(l)$ for finding easy inspection method. In this paper, therefore, the PD characteristics not only in $N_2(l)$ /PPLP® insulation system but also in $N_2(g)$ /PPLP® insulation system are investigated. Through the comparison of the PD characteristics under these environments, the appropriate pre-shipment test method will be proposed.

2. Materials and methods

Figures 1 and 2 show two types of samples for PD measurement used in this research. The sheet sample shown in Figure 1 consists of PPLP® layers with a hole simulating a butt gap. Samples which have 3, 5, 7, and 9 PPLP layers were used to assess surface/volume effects. To suppress surface discharge from the edge of the high voltage electrode, it was rounded and molded with silicon rubber. The detection electrode was divided from the grounded plate electrode with 1.5 mm thick insulator to measure the PD current. The cable sample shown in Figure 2 is a more practical model, which consists of a high voltage electrode as an inner cylinder, inner semi-conductor layers, PPLP® layers, outer semiconductor layers, and a grounded electrode as an outermost sheath. Samples which have 3, 9, 15 PPLP layers were tested, and the width of the detection electrode was 20 or 140 mm. The detection electrode of each cable sample was also separated to measure PD current. The surface area and the volume of butt-gaps in samples are listed in tables 1 and 2.

Figure 3 shows the experimental setup for measuring PD characteristics from 0.1 MPa to 1.0 MPa pressure $N_2(g)$ at room temperature. AC 50Hz high voltage was applied to the high voltage electrode of the sample. PD current was measured through measuring resistance (50Ω). In case of PD measurement in $N_2(l)$, thermal insulated tank was used, and PD current of a sample was measured by a current transformer (SE Technology Limited SCT-8). The measuring circuit is shown in Figure 4.

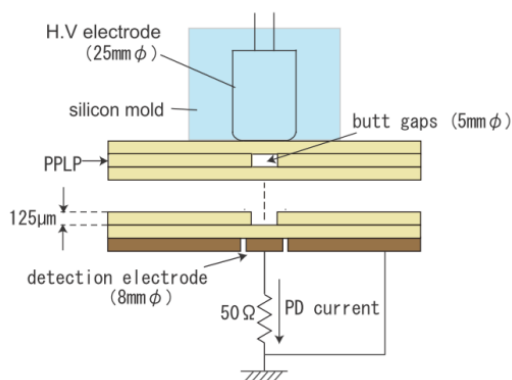


Figure 1. Configuration of sheet sample.

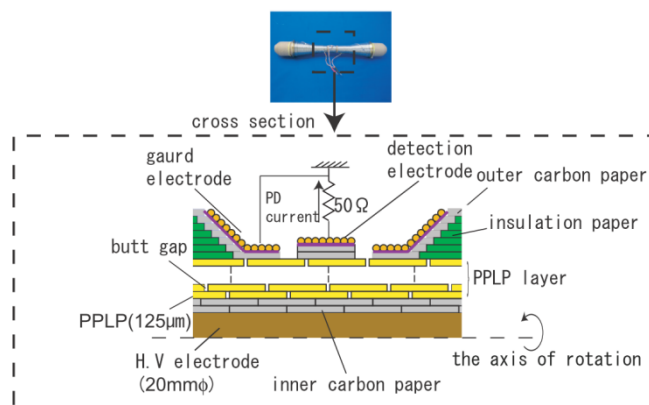


Figure 2. Configuration of cable sample.

Table 1. Surface area and volume of sheet model.

	Number of PPLP layers	Surface area (mm ²)	Volume (mm ³)
A	3	39.3	2.5
B	5	78.5	4.9
C	7	117.8	7.4
D	9	157.1	9.8

Table 2. Surface area and volume of cable model.

	Number of PPLP layers	Width of detection electrode (mm)	Surface area (mm ²)	Volume (mm ³)
E	3	20	400.7	25
F	15	20	2286.5	142.9
G	9	140	9009.3	563.1
H	15	140	16005.1	1000.3

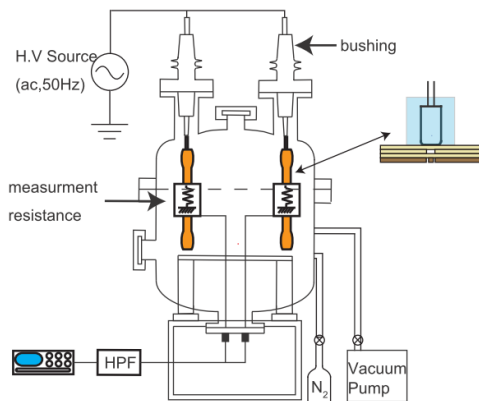


Figure 3. Experimental setup for $N_2(g)$.

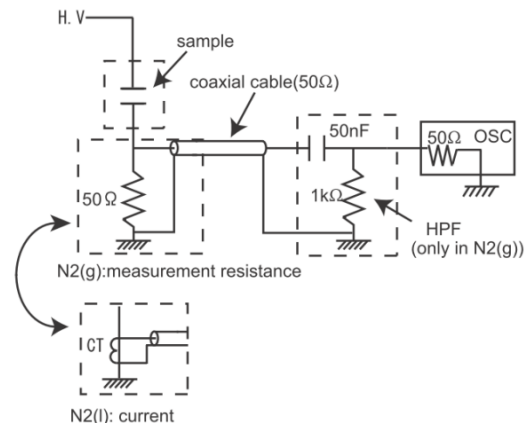


Figure 4. Measuring circuit.

3. Results and discussion

PD inception electric field (PDIE) and PD extinction electric field (PDEE) in $N_2(l)$ and $N_2(g)$ were measured. PDIE was obtained from Q - E characteristics *i.e.* the relationship between the PD charge amount (Q) and the applied electric field, with increasing applied electric field (E). In the same manner, PDEE was obtained with decreasing applied electric field. In this paper, PDIE and PDEE were defined as the electric field where Q takes threshold charge of 25 pC in Q - E curve. The charge amount of PD in $N_2(g)$ was obtained by integrating PD current waveform monitored by an oscilloscope. On the other hand, that in $N_2(l)$ was derived by the peak value of the current waveform, which was calibrated by measuring a mock PD-current waveform generated by a pulse generator (Nihon Keisokuki Seizosho co,ltd NPG-2).

Typical PD current waveforms in 1.0 MPa $N_2(g)$ are shown in Figure 5. The pulse width of the PD current waveform becomes shorter with the increase of $N_2(g)$ pressure, and the pulse width of PD current waveform in 1.0 MPa $N_2(g)$ is 5 – 10 ns. Figure 6 shows PD characteristics in 1.0 MPa $N_2(g)$. The electric fields in butt gap, E_{gap} , and the averaged applied electric field to the sample, E_{ave} , are expressed in this figure. E_{gap} [kVp/mm] were calculated from the peak applied voltage taking the relative permittivity of PPLP and N_2 into account, and E_{ave} [kVrm/mm] were obtained by simply dividing applied voltage by the sample thickness. As shown in Figure 6, Q - E curves are linear in semi logarithmic scale graphs, *i.e.*, the PD charge amount changes exponentially with the applied electric field. This tendency is observed both in $N_2(l)$ and $N_2(g)$ for every tested pressure with any samples.

Figure 7 shows the pressure dependence of PDIE and PDEE. Any significant difference between PDIE and PDEE aren't observed neither in $N_2(l)$ nor $N_2(g)$. PDIE and PDEE in $N_2(g)$ increase lineally with the gas pressure, on the other hand, PDIE and PDEE in $N_2(l)$ are saturated with the pressure at 0.3 MPa.

Figure 8 shows the PDIE with various volume and surface area of butt gap. In 1.0 MPa $N_2(g)$, PDIE decreases linearly with the volume V of butt gaps for $V < 1000 \text{ mm}^3$ and almost constant for $V > 1000 \text{ mm}^3$. In Figure 8, PDIE in 0.2 MPa $N_2(l)$ is also plotted. According to the paper by Hayakawa et al. [3], PDIE in $N_2(l)$ decreases for $V < 100 \text{ mm}^3$ and keeps constant for $V > 100 \text{ mm}^3$. The broken line in Figure 8 is drawn based on this report.

The converged values of PDIE in $N_2(g)$ with sufficiently large-volume butt gaps are compared to those in $N_2(l)$. Figure 9 shows the ratio of PDIE in $N_2(g)$ to that in 0.2 MPa $N_2(l)$, hereafter which is denoted as k , as a function of pressure of $N_2(g)$. The suffix "ave" and "gap" denote the values calculated with PDIEs expressed in the averaged field intensity across the sample and the field intensity in the butt gap, respectively. As shown in this figure, k increases with the gas pressure and k_{ave} reaches 0.3 in 1.0 MPa $N_2(g)$. This means that, subject to E_{ave} is comparable to the PDIE of $N_2(l)$, a PD shall occur at the gap in $N_2(g)$ at room temperature when 0.3 E_{ave} is applied.

4. Conclusions

In this paper, PDIE and PDEE of $N_2(l)$ /PPLP and $N_2(g)$ /PPLP composite insulation systems are investigated under 0.1 MPa to 0.3 MPa $N_2(l)$ and 0.1 MPa to 1.0 MPa $N_2(g)$ environment. The main conclusions are summarized as follows.

- (1) There is little difference between PDIE and PDEE in $N_2(l)$ and $N_2(g)$.
- (2) In $N_2(g)$, PDIE decreases linearly with the volume of butt gaps while the volume V is smaller than 1000 mm^3 , and keeps almost constant when V is larger than 1000 mm^3 .
- (3) The ratio of PDIE in $N_2(g)$ to that in 0.2 MPa $N_2(l)$ increases with the gas pressure and the ratio of E_{ave} reaches 0.3 in 1.0 MPa $N_2(g)$.

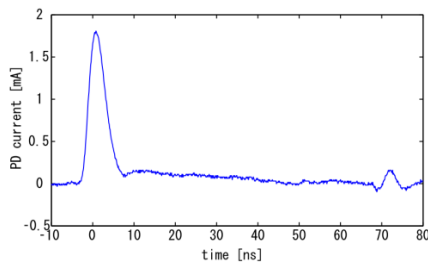


Figure 5. PD current waveform of cable model E in 1.0 MPa $N_2(g)$.

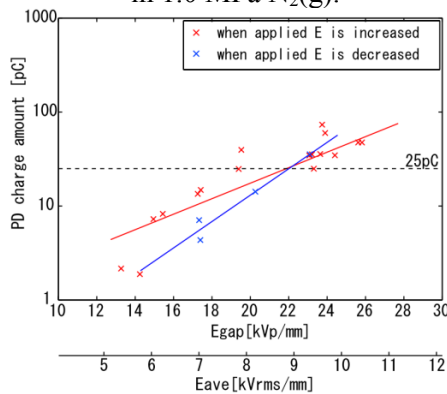


Figure 6. PD charge amount vs. applied electric field of cable model E in 1.0 MPa $N_2(g)$.

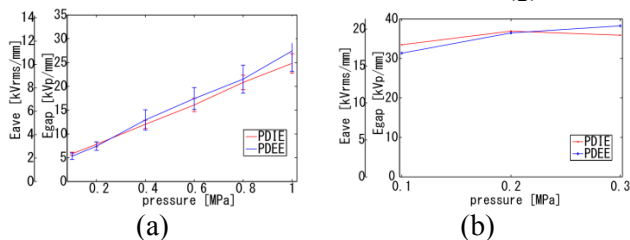


Figure 7. Plots of PDIE and PDEE of cable model E as a function of pressure (a) $N_2(g)$, (b) $N_2(l)$.

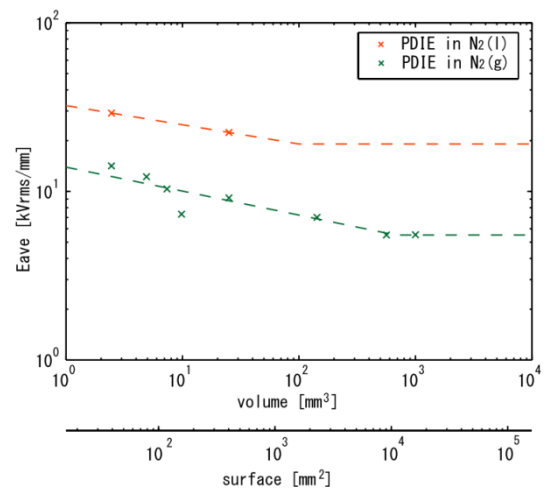


Figure 8. Volume/surface effect of PDIE in $N_2(l)$ and $N_2(g)$.

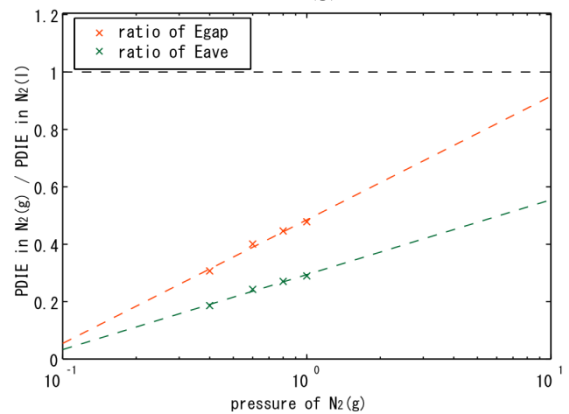


Figure 9. Estimated curve of the ratio of PDIE in $N_2(g)$ to PDIE in 0.2 MPa $N_2(l)$ as a function of gas pressure.

References

- [1] Ueda K, Tsukamoto O, Nagaya S, kimura H and Akita S 2003 *IEEE Trans. Applied Superconductivity*. **13** NO.2 1946-51
- [2] Rezaeifar F, Suzuki Y, Kumada A, Hidaka K, Masuda T and Nishimura T 2010 *IEEE Trans. Dielectrics and Electrical Insulation*. **17**, No. 6 1747-53
- [3] Hayakawa N, Yamaguchi R, Kojima H, Endo F and Okubo 2008 *IEEE Inter. Confe. On. Dielectric Liquids. ICDL 2008*. pp.1-4